Earth and Planetary Science Letters 361 (2013) 195–207

Contents lists available at SciVerse ScienceDirect

Earth and Planetary Science Letters

journal homepage: www.elsevier.com/locate/epsl

Crustal eclogitization and lithosphere delamination in orogens

Neil J. Krystopowicz [a], Claire A. Currie [b,*]

[a] Department of Earth and Atmospheric Sciences, University of Alberta, Edmonton, AB, Canada
[b] Department of Physics, 4-181 CCIS, University of Alberta, Edmonton, AB, Canada T6G 2E1

ARTICLE INFO

Article history:
Received 11 June 2012
Received in revised form
25 September 2012
Accepted 27 September 2012
Editor: Y. Ricard
Available online 22 December 2012

Keywords:
orogen
delamination
lithosphere removal
eclogite
numerical model

ABSTRACT

Many orogens, including the Central Andes and Himalayas, are characterized by wide areas that have undergone upper crustal shortening and surface uplift. The behaviour of the deep lithosphere is poorly constrained, and in some mountain belts, lower crust and mantle lithosphere appear to have been removed through delamination during orogen development. Thermal–mechanical numerical models demonstrate that as crust thickens during shortening, the lowermost crust may undergo metamorphic eclogitization, which increases its density. Even a small density increase (7% or more) causes shortening to localize above the eclogitic crustal root, promoting the development of thick lithosphere in this area which is then prone to gravitational removal. Complete removal of orogen mantle lithosphere occurs if the eclogitized lower crust is weak enough to allow full detachment of negatively buoyant mantle lithosphere; this can occur even if the lower crust is less dense than the mantle. The onset of delamination may be determined by the hydration state of the lower crust, as the presence of water promotes eclogitization and significantly reduces rock strength. Two distinct styles of delamination are observed: (1) retreating delamination in which weak mantle lithosphere rolls back and peels away from the crust, producing a contemporaneous migration of crustal thickening, surface uplift and magmatism, and (2) stationary delamination in which strong lithosphere separates from the weak lower crust and slides into the deep mantle at a stationary detachment point, followed by widespread crustal deformation and magmatism.

1. Introduction

During orogenesis, shortening produces thick (> 50 km) continental crust and corresponding high elevations that characterize orogens such as the Central Andes and Himalayas. The behaviour of the lower crust and mantle lithosphere remains poorly constrained. Shortening of the upper crust should be accompanied by thickening of the deeper lithosphere. However for many orogens, geophysical and geological observations indicate that mantle lithosphere is anomalously thin or absent.

Seismic studies of the Central Andes show low velocities and high attenuation in the shallow mantle of the eastern Altiplano Plateau (Beck and Zandt, 2002) and throughout the Puna Plateau (Schurr et al., 2006). These data imply high temperatures and the absence of a lithospheric lid for much of the orogen. Higher mantle velocities are observed in some areas, such as the central Altiplano, indicating regions of locally thicker lithosphere (Beck and Zandt, 2002). Seismic data also show that the crust is 50–70 km thick, with velocities that are consistent with a felsic composition, suggesting that the mafic lower crust has been removed (Beck and Zandt, 2002). Seismic data reveal present-day lithosphere structure but does not constrain the timing of removal. There is mounting evidence to indicate that lithosphere loss occurred during Cenozoic orogen shortening, including observations of rapid surface uplift, voluminous magmatism, and a change in crustal stress from compression to extension (e.g., Kay and Kay, 1993; Garzione et al., 2008; Kay and Coira, 2009). Similar observations have been used to infer lithosphere removal in other mountain belts, such as the Tibetan Plateau (e.g., England and Houseman, 1989; Jimenez-Munt et al., 2008), East Anatolian Plateau (e.g., Keskin, 2003; Sengor et al., 2003), Eastern Carpathians (e.g., Knapp et al., 2005; Fillerup et al., 2010), Sierra–Nevada region (e.g., Ducea and Saleeby, 1998), and Varsican orogen (e.g., Gutierrez-Alonso et al., 2011), suggesting that this is an important process in orogen evolution.

Mantle lithosphere, being cooler and therefore denser than the underlying material, is gravitationally unstable and susceptible to removal. One mechanism is convective removal via Rayleigh–Taylor-type (RT) instability ("drip") (Houseman et al., 1981), possibly initiated by shortening-induced perturbation of the lithosphere. However, most studies conclude that removal is generally limited to the lowermost lithosphere, owing to the strong temperature-dependence of typical mantle rheologies (e.g., Buck and Toksoz, 1983; Conrad and Molnar, 1999). An alternate

* Corresponding author. Tel.: +1 780 492 1062; fax: +1 780 492 0714.
E-mail address: claire.currie@ualberta.ca (C.A. Currie).

0012-821X/$ - see front matter © 2012 Elsevier B.V. All rights reserved.
http://dx.doi.org/10.1016/j.epsl.2012.09.056

removal mechanism is delamination, which involves peeling of mantle lithosphere along the Moho (Bird, 1979), and by definition, removes the entire mantle lithosphere. Delamination requires a weak zone in the deep crust (Meissner and Mooney, 1998), which may be related to high Moho temperatures (e.g., Morency and Doin, 2004) or rheological weakness associated with hydration (e.g., Schott and Schmeling, 1998).

In many modelling studies, delamination is induced using a prescribed weak layer (e.g., Schott and Schmeling, 1998, Gogus and Pysklywec, 2008a, 2008b; Valera et al., 2011; Bajolet et al., 2012). These studies provide insights into the consequences of lithosphere removal on surface topography, crustal deformation, and thermal structure but do not address the factors leading to delamination. Numerical models of Morency and Doin (2004) demonstrate that delamination can develop dynamically through localized lithosphere thinning associated with mantle convection. Alternatively, models of continental collision show that delamination may be induced by retreat of high density subducting lithosphere (Beaumont et al., 2006; Gray and Pysklywec, 2012), where decoupling is enhanced if the plate boundary is rheologically weak (Faccenda et al., 2009; Ueda et al., 2012).

In this study, we consider the role of lower crustal eclogitization in triggering delamination. Prograde metamorphism of the deep crust as it shortens and thickens may produce an eclogitized crustal root. The density of the root depends on its composition, extent of eclogitization, and local pressure and temperature conditions. For a mafic composition, the eclogitized root can be denser than the underlying mantle and thus it is prone to foundering (e.g., Kay and Kay, 1993). Numerical models confirm that high density eclogite decreases RT instability times (Jull and Kelemen, 2001), affects orogen evolution if the crust is decoupled from the mantle (Doin and Henry, 2001) and can lead to delamination (e.g., Sobolev and Babeyko, 2005; Le Pourhiet et al., 2006).

Here, we use thermal–mechanical numerical models to assess the effect of eclogitization of the lower crust during orogen shortening. We systematically examine variations in eclogite density and strength of the crust and mantle lithosphere to understand the conditions required for delamination. In contrast to some previous studies, models do not include an imposed lithosphere thickness perturbation or prescribed eclogite layer. Instead, eclogitization and gravitational instability develop self-consistently during model evolution. Our study focuses on metamorphic eclogitization of thickened crust as the orogen shortens. Eclogitized crust may also be produced through igneous processes, whereby magmatic differentiation leaves a mafic residue in the deep crust (e.g., Kay and Kay, 1993; Jull and Kelemen, 2001; Kay and Coira, 2009). In this case, there may be no relationship between orogen shortening and eclogite formation.

2. Numerical modelling approach

2.1. Methods and model geometry

Two-dimensional numerical models are used to study the behaviour of continental lithosphere during shortening. The coupled thermal–mechanical evolution of the lithosphere–upper mantle system is modelled using the SOPALE code, which has been widely applied to studies of lithosphere dynamics (e.g., Pysklywec and Beaumont, 2004; Beaumont et al., 2006; Gogus and Pysklywec, 2008a; 2008b; Warren et al., 2008; Currie and Beaumont, 2011; Gray and Pysklywec, 2012). Arbitrary Eulerian–Lagrangian finite element techniques are used to solve the equations of mass conservation, force balance and energy balance, under the assumptions of plain strain, incompressibility and zero Reynolds number. Mechanical and thermal calculations are performed on an Eulerian mesh that stretches vertically to conform to the top model boundary, which is a free surface. Material properties are tracked on a Lagrangian mesh, with additional Lagrangian tracer particles which are advected with the model velocity field. Full details of the numerical method and model parameterization are given by Fullsack (1995) and Beaumont et al. (2006).

The model domain has a width of 1200 km and extends from the Earth's surface to 660 km depth (Fig. 1a). The 100 km thick continental plate consists of 25 km upper-mid crust, 15 km lower crust, and 60 km mantle lithosphere. The crust is divided into an 850 km wide weak region (orogen) with strong blocks on either side. This geometry replicates the orogenic vise model, in which shortening occurs within a zone of inherited weakness (Ellis et al., 1998). For example, shortening in the Central Andes is confined to accreted and rifted terranes that are bounded by strong forearc on the west and Brazilian craton on the east (e.g., Oncken et al. 2006). Similarly, the wide area of Himalayan deformation has been related to pre-existing weakness associated with high temperatures (Molnar and Tapponnier, 1981). The Eulerian mesh has 120 elements horizontally (10 km width) and 108 elements vertically, with 56 elements in the upper 140 km (2.5 km height) and 52 elements below (10 km height). Models with a higher resolution mesh give comparable results (see Supplementary material).

Shortening is produced by introducing strong continental lithosphere through the right-hand model boundary at a rate of 1 cm/yr, comparable to the Cenozoic shortening rate of the Central Andes (e.g., Oncken et al., 2006). Shortening is inferred to be related to plate boundary forces originating to the right of the model domain (c.f., Doin and Henry, 2001; Beaumont et al., 2006). Within the domain, materials evolve dynamically in response to boundary conditions and internal buoyancy forces.

2.2. Material properties and model boundary conditions

All model materials have a viscous-plastic rheology. Frictional-plastic deformation follows a Drucker–Prager yield criterion:

$$(J_2')^{1/2} = c_0 \cos\phi_{eff} + P \sin\phi_{eff} \quad (1)$$

where J'_2 is the second invariant of the deviatoric stress tensor σ'_{ij} ($2J'_2 = \sigma'_{ij}\sigma'_{ij}$), c_0 is cohesion, ϕ_{eff} is the effective internal angle of friction, and P is the pressure. Frictional-plastic deformation is modelled using an effective viscosity that places the state of stress on yield (Fullsack, 1995; Willett, 1999). Materials undergo frictional-plastic strain softening where ϕ_{eff} decreases from 15° to 2° over accumulated strain (I'_2) of 0.5–1.5 (e.g., Warren et al., 2008 and references therein).

At stresses below frictional-plastic yield, materials deform viscously in power law creep:

$$\eta_{eff} = f(B^*)(\dot{I}_2')^{(1-n)/2n} \exp\left(\frac{Q+PV^*}{nRT_K}\right) \quad (2)$$

where η_{eff} is effective viscosity, f is a scaling factor (see below), $\dot{I}'_2$ is the second invariant of the strain rate tensor $\dot{\varepsilon}_{ij}$ ($2\dot{I}'_2 = \dot{\varepsilon}_{ij}\dot{\varepsilon}_{ij}$), R is the universal gas constant, and T_K is the absolute temperature. The rheological parameters, B^*, n, Q, and V^*, are the pre-exponential factor, the stress exponent, the activation energy and the activation volume, respectively.

Rheological parameters are given in Table 1. The laboratory-derived viscous flow laws of wet quartzite (WQ, Gleason and Tullis, 1995), dry Maryland diabase (DMD, Mackwell et al., 1998), and wet olivine (WO, Karato and Wu, 1993) are used for the upper-mid crust, lower crust and mantle, respectively. Following previous studies (e.g., Beaumont et al., 2006), a scaling factor (f) is

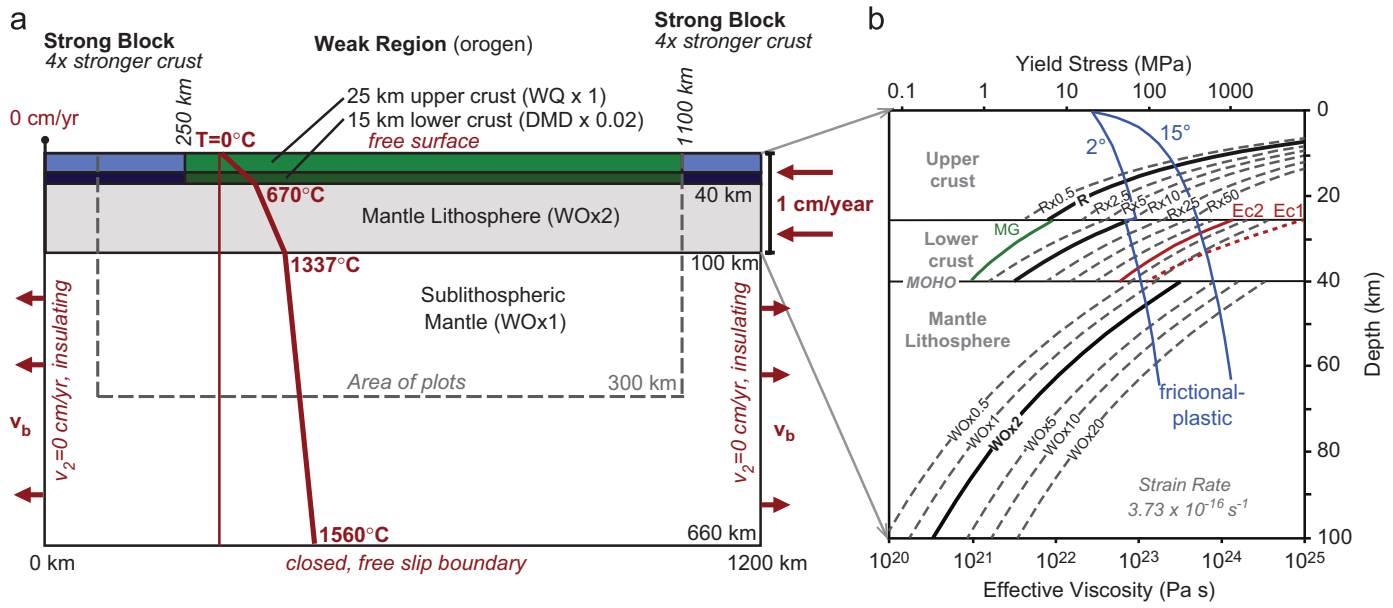

Fig. 1. (a) Initial model geometry and thermal–mechanical boundary conditions. V_b is a small uniform outflux velocity for the sublithospheric mantle that balances the influx of lithosphere. The initial thermal structure is shown with the red geotherm. Material parameters are given in Table 1. WQ=wet quartzite (Gleason and Tullis, 1995); DMD=dry Maryland diabase (Mackwell et al., 1998); WO=wet olivine (Karato and Wu, 1993). (b) Lithosphere strength profiles for orogen lithosphere. Blue lines show frictional-plastic yield stress for unsoftened ($\phi=15^\circ$) and softened ($\phi=2^\circ$) material. Black lines show effective viscosity for viscous materials, calculated using the initial thermal structure and strain rate of 3.73×10^{-16} s^{-1}, based on the starting orogen width (850 km) and shortening rate (1 cm/yr). Note that strain rate varies during model evolution. The thick black line shows the viscous strength for the reference model (R), and dashed lines show variations in strength tested in this study (see text for details). In the lower crust, strength profiles for mafic granulite (MG, green line; Wang et al., 2012) and dry eclogite are shown for comparison to the DMD rheology. Eclogite profiles use the rheological parameters of Jin et al. (2001) (Ec1, dotted red line) and Zhang and Green (2007) (Ec2, solid red line); eclogite is not stable at the initial lower crustal pressures. (For interpretation of the references to colour in this figure legend, the reader is referred to the web version of this article.)

Table 1
Material parameters used in the reference models (Model 1 and Model 2).

	Upper-mid crust	Lower crust	Mantle lithosphere	Sublithospheric mantle
Plastic rheology				
c_0 (MPa)	20	0	0	0
ϕ_{eff}	15–2°	15–2°	15–2°	15–2°
Viscous rheology				
f	1	0.02	2	1
A^* (Pa^{-n} s^{-1})	1.10×10^{-28}	5.05×10^{-28}	3.91×10^{-15}	3.91×10^{-15}
B^* (Pa s$^{1/n}$)[a]	2.92×10^{6}	1.91×10^{5}	1.92×10^{4}	1.92×10^{4}
n	4.0	4.7	3.0	3.0
Q (kJ mol^{-1})	223	485	430	430
V^* (cm^3 mol^{-1})	0	0	15	15
Thermal parameters[b]				
k (W m^{-1} K^{-1})[c]	2.25	2.25	2.25	62.5
A (μW m^{-3})	1.0	0.4	0.0	0.0
c_p (J kg^{-1} K^{-1})	750	750	1250	1250
Density[d]				
ρ_0 (kg m^{-3})	2800	3000	3250	3250
T_0 (°C)	627	627	1344	1344
Eclogite ρ_0 (kg m^{-3})[e]	–	3450	–	–
α (K^{-1})	3.0×10^{-5}	3.0×10^{-5}	3.0×10^{-5}	3.0×10^{-5}

[a] $B^*=(2^{(1-n)/n}3^{-(n+1)/2n})A^{*-1/n}$; the term in brackets converts the plane strain pre-exponential factor from uniaxial laboratory experiments (A^*) to the tensor invariant state of stress of the numerical models.
[b] k is the thermal conductivity, A is the radioactive heat production and c_p is the specific heat.
[c] Thermal conductivity used for temperatures below 1337 °C; at higher temperatures, the thermal conductivity linearly increases from 2.25 W m^{-1} K^{-1} to 62.5 W m^{-1} K^{-1} at 1377 °C.
[d] Temperature dependent density: $\rho(T)=\rho_0\,[1-\alpha(T-T_0)]$, where ρ_0 is the reference density at temperature T_0 and α is the volumetric thermal expansion coefficient.
[e] Eclogitized lower crust not included in Model 1.

used to linearly scale the viscosity of model materials relative to the laboratory rheologies, as a means of examining model sensitivity to material strength owing to variations in thermal structure, composition or degree of hydration, and uncertainties in the published parameters. In the reference models (Models 1 and 2), the orogen upper-mid crust has $f=1$ and lower crust has $f=0.02$. The crustal layers in the adjacent vises are 4 times stronger; experiments show this contrast is sufficient to focus

deformation within the weak region. The entire model has uniform mantle lithosphere with $f=2$ (WO $\times$ 2), making it two times stronger than the sublithospheric mantle (WO $\times$ 1) to approximate a melt-depleted lithosphere.

Fig. 1b shows the strength profile for orogen lithosphere at the start of the models. The scaling factors for the orogen lithosphere (WQ $\times$ 1, DMD $\times$ 0.02, WO $\times$ 2) are five times less than those used by Currie and Beaumont (2011), as our goal is to examine shortening of weak lithosphere. In Section 5, we examine variations in crust and mantle strength over the range shown in Fig. 1b.

All materials have a temperature-dependent density (Table 1). The upper-mid and lower crust densities are 520 and 320 kg/m^3, respectively, less than mantle density at the same temperature. All mantle materials have the same compositional density, and thus density variations are solely due to temperature.

Radioactive heat productions of 1 μW/m^3, 0.4 μW/m^3, and 0 μW/m^3 are used for the upper-mid crust, lower crust, and mantle, respectively. In the lithosphere (temperature less than 1337 °C), all materials have a thermal conductivity of 2.25 Wm^{-1} K^{-1}. The thermal conductivity of sublithospheric mantle increases from 2.25 Wm^{-1} K^{-1} to 62.5 Wm^{-1} K^{-1}, over temperatures of 1337 °C to 1377 °C, above which it is constant. The enhanced conductivity simulates heat transport by marginally supercritical convection (Pysklywec and Beaumont, 2004), which is not explicitly modelled. This maintains an approximately constant mantle heat flow of 25 mW/m^2 and adiabatic temperature gradient in the sublithsopheric mantle.

Mechanical and thermal boundary conditions for the models are given in Fig. 1a. Models do not include surface erosion or sedimentation. At the lithosphere side boundaries, a continental geotherm is prescribed, based on the top (0 °C) and bottom (1560 °C) model temperatures and material thermal properties (Fig. 1a). As there are no lateral variations in properties, this geotherm also represents the initial thermal structure for the model domain, with surface heat flow of 56 mW/m^2 and temperatures of 670 °C at the Moho and 1337 °C at the base of the lithosphere.

3. Reference model with no eclogitization (Model 1)

Fig. 2 shows the evolution of Model 1 in which there is no crustal eclogitization. With convergence of the right-hand strong block, the weak crustal region undergoes symmetric pure shear shortening, resulting in lithosphere thickening and surface uplift. Although the entire mantle lithosphere has the same rheology, thickening is limited to the area with weak crust. By 50 Ma (500 km of shortening), the orogen has an ~80 km thick crust and a ~4 km elevation. The thickened mantle lithosphere is relatively stable, with only minor RT-type instabilities at its sides. These instabilities remove ~20 km of lithosphere, but thick lithosphere remains below the orogen.

Reasonable variations in crustal and mantle strength do not change the overall behaviour. Crustal strength has little effect on RT-type instabilities in the mantle lithosphere. A weaker mantle lithosphere undergoes instability earlier in model evolution, but in all cases, less than 30% of lithosphere is removed, owing to its temperature-dependent rheology. Although the shallow mantle lithosphere is cool and dense, it also has a high viscosity, which limits its susceptibility to RT-type removal (e.g., Buck and Toksoz, 1983; Conrad and Molnar, 1999). Thus, it is difficult to reconcile these models with observations of thinned orogenic lithosphere, unless mantle rheology has a much weaker temperature-dependence than given by laboratory studies (e.g., Gogus and Pysklywec, 2008a) or there is an additional destabilization mechanism.

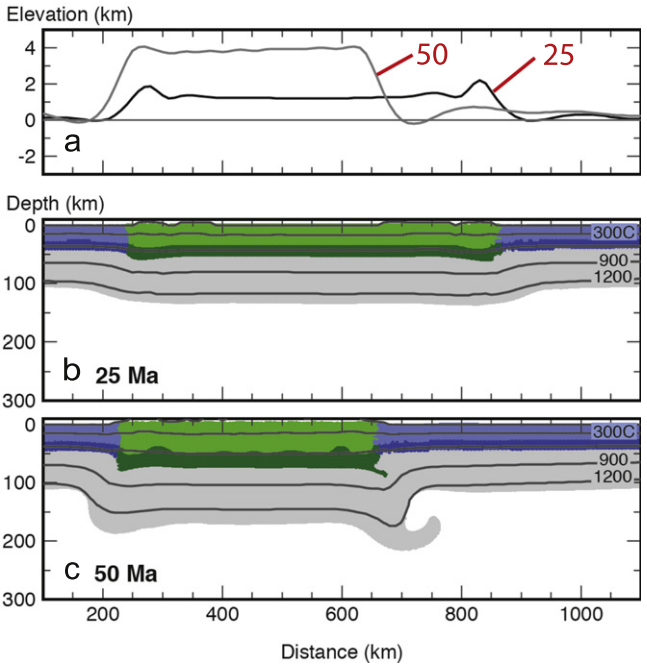

Fig. 2. Evolution of **Model 1**, in which there is no lower crustal eclogitization. (a) Surface topography (red numbers indicate model time in Ma), and model geometry at (b) 25 Ma and (c) 50 Ma after initiation of shortening. (For interpretation of the references to colour in this figure legend, the reader is referred to the web version of this article.)

4. Lower crustal eclogitization

4.1. Modelling approach

We now examine the effect of a density increase in thickened lower crust associated with metamorphic eclogitization. The eclogite stability field is defined using the basalt phase diagram of Hacker et al. (2003). Mafic continental crust has a similar stability field (e.g., Bousquet et al., 1997) (see Supplementary material). Material pressure–temperature conditions are tracked during model evolution, and as lower crust enters the eclogite stability field, its rheology and density change to those of eclogite, assuming no kinetic hindrance in the reaction. Two laboratory studies have examined the rheology of dry eclogite (Jin et al., 2001; Zhang and Green, 2007) and show that its strength is similar to that of dry Maryland diabase (Fig. 1b). Eclogitized rocks containing water may be much weaker (Zhang and Green, 2007). In this section, eclogitized crust has the same rheological properties as its protolith (i.e., DMD $\times$ 0.02). Variations in rheology are examined in Section 5.2.

The density of eclogitized crust depends on both its composition and extent of eclogitization. Studies indicate that eclogitized mafic crust can be 50–300 kg/m^3 more dense than mantle (e.g., Bousquet et al., 1997; Jull and Kelemen, 2001). There are also examples where eclogitized crust is less dense than mantle owing to either a more felsic composition or incomplete eclogitization (e.g., Bousquet et al., 1997, Austrheim, 1991). In nature, eclogitization occurs heterogeneously, resulting in localized zones of eclogite adjacent to unreacted crustal rocks (Austrheim et al., 1997). In our models, the properties of all lower crustal material within the eclogite stability field are modified. Thus, the assigned density values reflect the average density of rock containing both metastable granulite and eclogitized crust. We have tested eclogite-mantle density contrasts ranging from -200 kg/m^3 to $+130$ kg/m^3, corresponding to an increase in lower crustal density of 4–15% during eclogitization. Assuming densities of 3000 kg/m^3 for mafic granulite and 3500–3600 kg/m^3 for mafic

eclogite (Christensen and Mooney, 1995; Austrheim et al., 1997; Bousquet et al., 1997), the range of model densities reflects eclogitization of 20–90% of mafic lower crust. At the time of the phase change, the incompressibility condition in the mechanical calculation is relaxed, and a compressive force is applied to Eulerian elements that experience densification, producing a fractional volume reduction (Warren et al., 2008). This ensures that models remain in mass balance; failure to do so results in inaccurate buoyancy forces, which affects model evolution (Warren et al., 2008; Hetenyi et al., 2011).

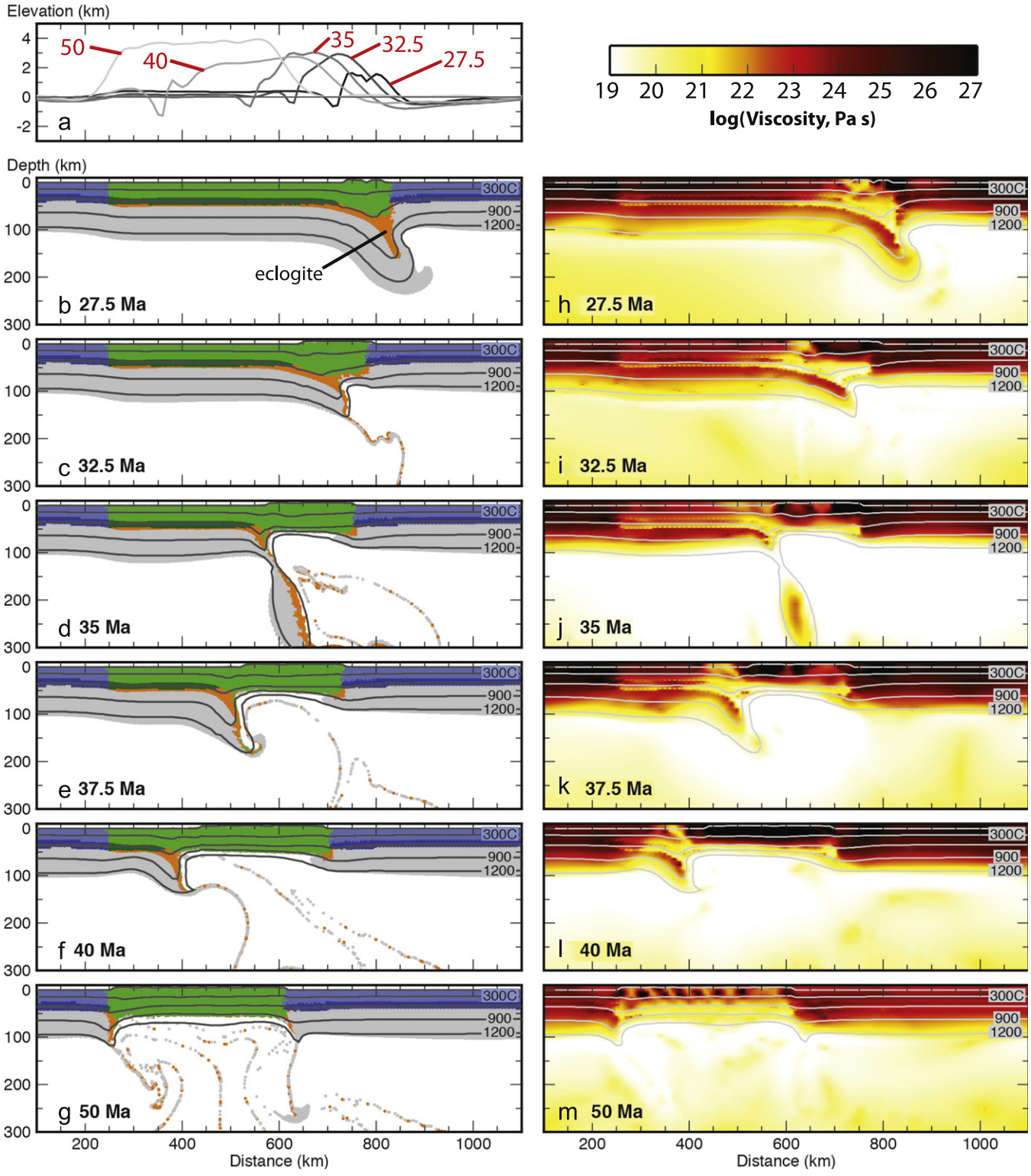

Fig. 3. Model 2 with the reference lithosphere strength and eclogitized lower crust (orange), which is 130 kg/m^3 denser than mantle. (a) Surface topography, (b–g) material distribution (colours as in Fig. 1a), and (h–m) viscosity structure at the given model times. This behaviour is classified as retreating delamination as lithosphere peels away from the crust at a retreating detachment point. The detached lithosphere undergoes episodic break-off during removal. (a) Elevation (km), (b,h) 27.5 Ma, (c,i) 32.5 Ma, (d,j) 35 Ma, (e,k) 37.5 Ma, (f,l) 40 Ma and (g,m) 50 Ma. (For interpretation of the references to colour in this figure legend, the reader is referred to the web version of this article.)

4.2. Reference model with eclogitization (Model 2)

Model 2 is identical to Model 1, except that it includes formation of eclogite that is 130 kg/m^3 more dense than mantle. With shortening and thickening, the deep orogenic crust undergoes eclogitization (Fig. 3b). The negative buoyancy of the eclogite root leads to localized shortening at the edges of the weak region, with stronger localization on the right-hand side owing to the incoming strong block (see Supplementary material). This results in crustal thickening and surface uplift above the root and underthrusting of orogen mantle lithosphere below the strong block. Numerical models of Hetenyi et al. (2011) show a similar feedback between eclogite formation and localization of deformation. In our models, the weak crust forms a low viscosity layer above the underthrust lithosphere (Fig. 3h). This allows the negatively buoyant lithosphere to roll-back and then break off at ~32.5 Ma (Fig. 3c), producing surface uplift of 1–1.5 km (Fig. 3a). Orogen lithosphere adjacent to the newly-created gap then begins to peel away from the crust at a detachment point that moves to the left; we call this retreating delamination (Fig. 3d–f). This process is enabled by the low viscosity lower crust, which decouples the lithosphere from the upper-mid crust (Fig. 3i–l). As the lithosphere delaminates, it breaks into pieces ~200 km long. Delamination is accompanied by migration of crustal shortening and thickening above the detachment point, with punctuated uplift events (~0.5 km) above areas of slab break-offs (Fig. 3a). A small basin develops in front of the migrating crustal wedge but disappears as the wedge encounters the left-hand strong block. By ~47.5 Ma, the orogen mantle lithosphere and lower crust have been removed, and the remaining crust undergoes pure shear shortening (Fig. 3g).

4.3. Variations in eclogite density

Eclogitized lower crust is a key factor that triggers delamination in Model 2; the equivalent model without eclogitization (Model 1) did not delaminate. As noted above, the density of eclogitized crust can vary with composition and degree of eclogitization. The high density in Model 2 reflects nearly complete eclogitization of mafic crust (e.g., Bousquet et al., 1997), whereas Model 1 represents no eclogitization (i.e., metastability). Fig. 4 (crustal strength R × 1) shows how variations in eclogite density affect delamination. As eclogite density decreases, a later onset and longer duration of delamination is observed, and break-offs involve longer slabs. Delamination occurs in models where eclogite is up to 100 kg/m^3 less dense than mantle (Model A1 in the Supplementary material). At lower densities, the orogen lithosphere thickens and experiences minor RT-type drips, similar to the behaviour seen in Fig. 2; wholesale mantle lithosphere removal does not occur.

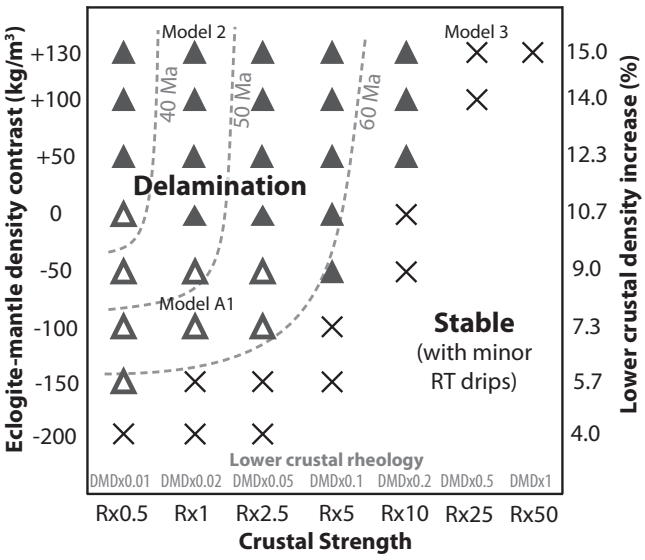

Fig. 4. Model behaviour for variations in crustal strength (relative to reference strength, R) and density contrast between eclogitized crust and mantle (at the same temperature). Grey labels are the lower crustal rheology as a scaling of the dry Maryland diabase rheology (DMD). The lower crustal density increase (in %) during eclogitization is also given. Crosses are models that remain stable throughout model evolution and triangles are models which exhibit delamination; solid triangles indicate retreating delamination and open triangles indicate retreating delamination followed by stationary delamination. Dashed lines show the time (since initiation of shortening) for removal of >90% of orogen mantle lithosphere.

5. Variations in crust and mantle strength

In the above models, the deep crust is weak, which promotes decoupling of the crust and mantle (Fig. 3h–m). The viscous strength of both the crust and mantle lithosphere is expected to vary with changes in composition, degree of hydration, and temperature, with increased strength for more mafic, drier or cooler conditions. In this section, we examine changes in crust and mantle strengths by varying the scaling factor f in Eq. (2).

5.1. Crustal strength (Model 3)

Crustal strength variations are studied by changing f for both upper-mid and lower crust, such that their relative strength remains constant. We report this as a scaling of the reference rheology (R) of Model 2, and crustal strength variations from R × 0.5 to R × 50 are tested (Fig. 1b). For example, R × 10 represents crust that is 10 times stronger than the Model 2 crust (i.e., f=10 for upper-mid crust, f=0.2 for lower crust).

Fig. 4 shows how variations in crustal strength and eclogite density affect behaviour. Delamination is observed in models in which the crust is weak and eclogite has a relatively high density. The timescale for delamination decreases with decreasing crustal strength and increasing eclogite density. For the weakest crust (R × 0.5), delamination is observed for eclogite densities up to 150 kg/m^3 less than the mantle density. The minimum density for delamination increases with increasing crustal strength. Note that the lower crust is cooler than the mantle and therefore some compositional buoyancy is offset by the lower temperatures.

Models with low density eclogite and/or a strong crust do not exhibit delamination. If the crust is weak, the orogen exhibits pure shear thickening and minor RT-type drips (e.g., Fig. 2). At higher strength, it is more difficult to shorten the crust through pure shear. Fig. 5 shows the behaviour of Model 3, in which crustal strength is R × 25 and eclogite is 130 kg/m^3 denser than mantle. The crust initially deforms by minor buckling, and by 27.5 Ma, the orogen lithosphere underthrusts the right-hand strong block, with limited crustal thickening. The underthrust lithosphere is gravitationally unstable, and its tip detaches at 42.5 Ma. With continued shortening, underthrusting develops at the left-hand side of the orogen (Fig. 5d). Overall, the crust and mantle are coupled throughout model evolution, owing to the high viscosity of the lower crust (Fig. 5e–g), and removal occurs through RT-type drips of mantle lithosphere.

5.2. Eclogite rheology (Models 4 and 5)

The previous models assume that lower crustal rheology does not change during eclogite formation. However, eclogitization

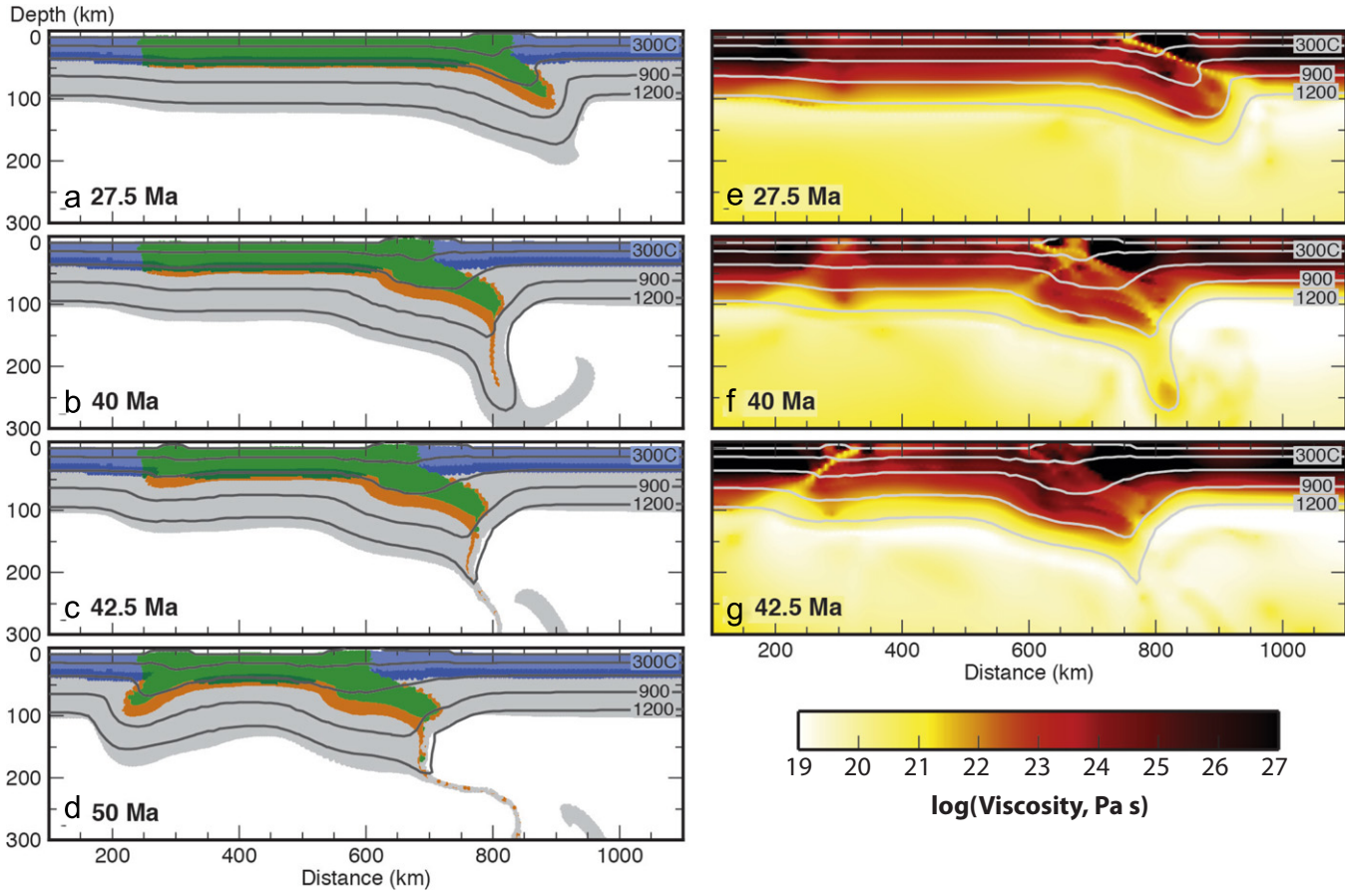

Fig. 5. (a–d) Material distribution and (e–g) viscosity structure of **Model 3**, in which the crust is 25 times stronger than that in **Model 2**; all other parameters are the same. With the stronger crust, shortening is primarily accommodated by underthrusting. The orogen crust and mantle are strongly coupled, preventing delamination. (a,e) 27.5 Ma, (b,f) 40 Ma, (c,g) 42.5 Ma and (d) 50 Ma.

may lead to strengthening or weakening of lower crust. In Model 4, we test the effect of strong eclogitized crust, using the Model 2 parameters and introducing a rheological change for eclogitized crust from the initial DMD $\times$ 0.02 rheology to the eclogite rheology of Jin et al. (2001) (i.e., the stronger eclogite rheology in Fig. 1b). This corresponds to a strength increase by a factor of $\sim$50, which may represent dehydration as lower crust eclogitizes. In contrast to Model 2 which readily delaminates, the strong eclogitized crust stabilizes the orogen (Fig. 6a–c). As the orogen lithosphere thickens and underthrusts, small RT-type drips occur at its edge, but the lower crust and mantle remain coupled, resulting in a thick orogen lithosphere. Only late in model evolution does delamination begin, with detachment at the base of the weak upper-mid crust (Fig. 6d).

Conversely, eclogitization may result in lower crustal weakening, possibly related to the presence of water or weak minerals, such as omphacite (Austrheim, 1991; Leech, 2001; Jackson et al., 2004; Zhang and Green, 2007). Model 5 uses the strong R $\times$ 25 crust of Model 3 but includes a weakening of lower crust by a factor of 25 as it eclogitizes, to test the effect of extreme weakening. As seen in Model 3, shortening is mainly accommodated by underthrusting (Fig. 6e). However, in Model 5, the weak eclogite promotes decoupling of the crust and mantle, allowing full removal of the underthrust lithosphere. Continued shortening produces outward growth of a thick upper crust through underthrusting, accompanied by removal events involving the entire mantle lithosphere (Fig. 6f–h). The spatial extent of removal is limited to the area with weak eclogitized crust.

Models 4 and 5 demonstrate that lower crustal strength is an important factor that controls the onset of delamination. Significant lower crustal weakening during eclogitization promotes lithosphere removal, but Model 5 suggests that the lower crust must be fairly weak prior to metamorphism to enable rapid delamination. A weak crust is also needed to allow initial shortening of the orogen.

5.3. Mantle lithosphere strength (Model 6)

We have tested variations in mantle lithosphere strength by scaling the base wet olivine (WO) rheology by $f=0.5$ to $f=20$; the reference model has $f=2$. Fig. 7 summarizes model behaviour for variations in crustal and mantle lithosphere strength, using an eclogite-mantle density contrast of $+130\ \mathrm{kg/m^3}$. Overall, the propensity for delamination is primarily controlled by crustal strength and eclogite density. There is a weak dependence on mantle lithosphere strength, with delamination of strong mantle requiring a weaker crust.

We find that the style of delamination varies with mantle lithosphere strength. At low strength, retreating delamination is observed, where the lithosphere detaches through roll-back. As mantle lithosphere becomes weaker than WO $\times$ 2, removal still occurs along a deep crustal detachment layer, but there is a gradation from block-like delamination to a more "drippy" appearance of the detached lithosphere (Model A2 in the Supplementary material).

At higher mantle lithosphere strength, there is an abrupt transition to what we have termed "stationary delamination". Fig. 8 shows the evolution of Model 6, which uses the same parameters as Model 2, but the mantle lithosphere is five times stronger (WO $\times$ 10). Shortening occurs at the sides of the weak region, producing surface

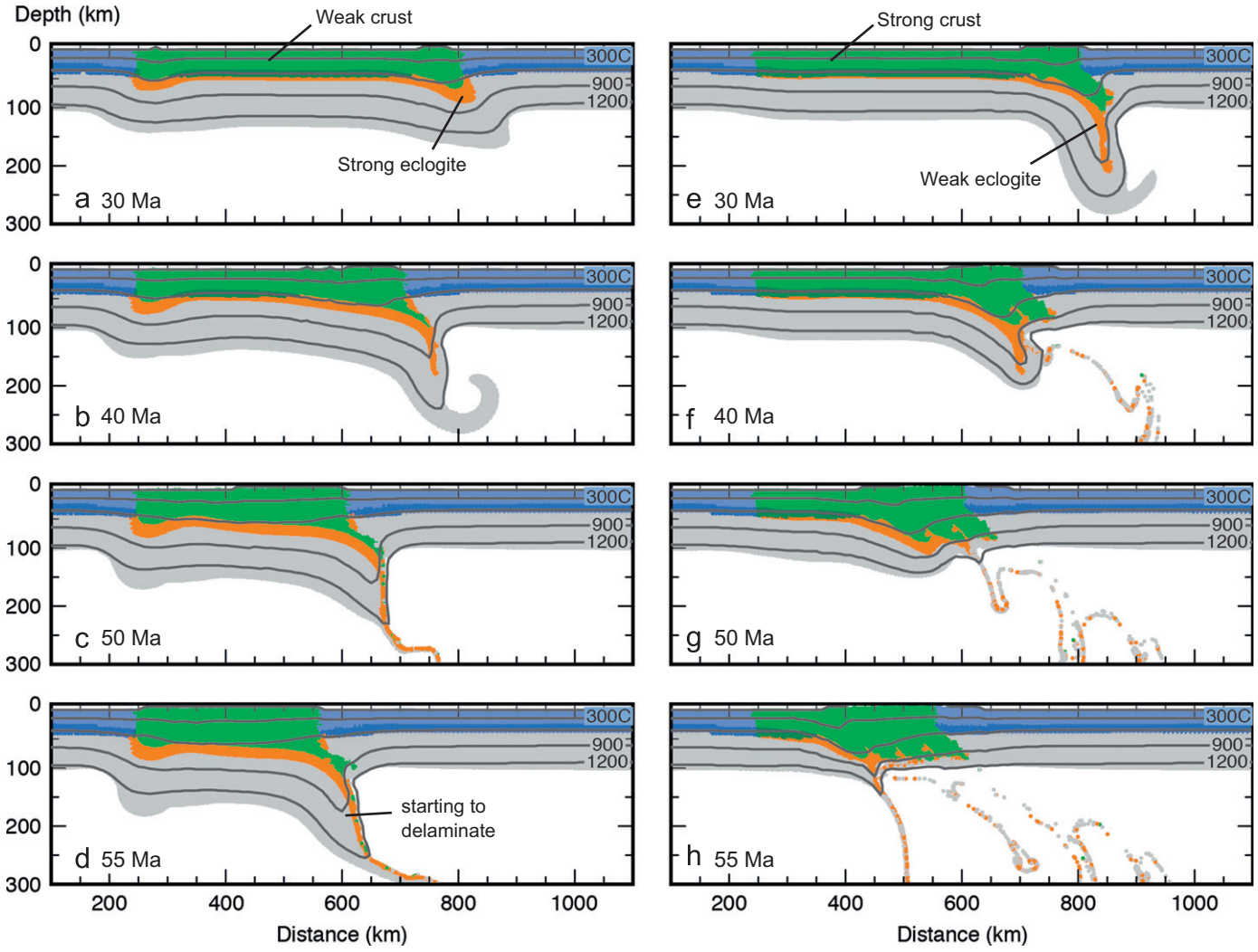

Fig. 6. (a–d) Evolution of **Model 4**, which has a weak crust (R × 1). During eclogitization, the lower crust rheology changes to that of dry eclogite (Jin et al., 2001), corresponding to a ~50 × strength increase. As a result, eclogitized crust and mantle are strongly coupled and delamination is suppressed until late in model evolution. (e–h) Evolution of **Model 5**, which has a strong crust (R × 25). During eclogitization, the strength of lower crust decreases by a factor of 25. This allows removal of mantle lithosphere and eclogitized lower crust, but only in the region of the eclogite root. (a,e) 30 Ma, (b,f) 40 Ma, (c,g) 50 Ma and (d,h) 55 Ma.

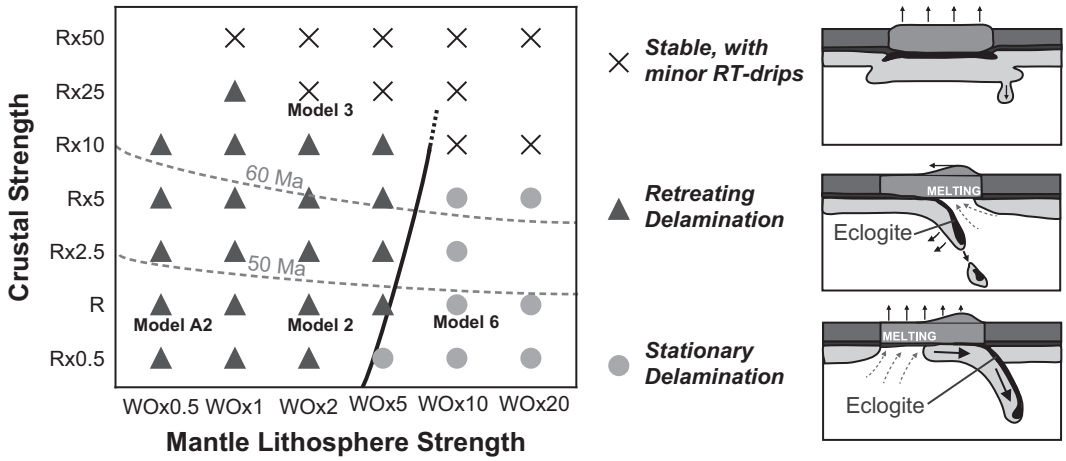

Fig. 7. Model behaviour for variations in orogen lithosphere strength in models that include lower crustal eclogitization. Eclogitized crust has a density that is 130 kg/m^3 greater than that of the mantle. Crustal strength is varied by linearly scaling the viscous rheology of the upper-mid and lower crust relative to the reference rheology (R). Mantle strength variations are reported as a linear scaling of the wet olivine (WO) rheology of Karato and Wu (1993). Dashed lines indicate the time (since initiation of shortening) for removal of > 90% of orogen mantle lithosphere.

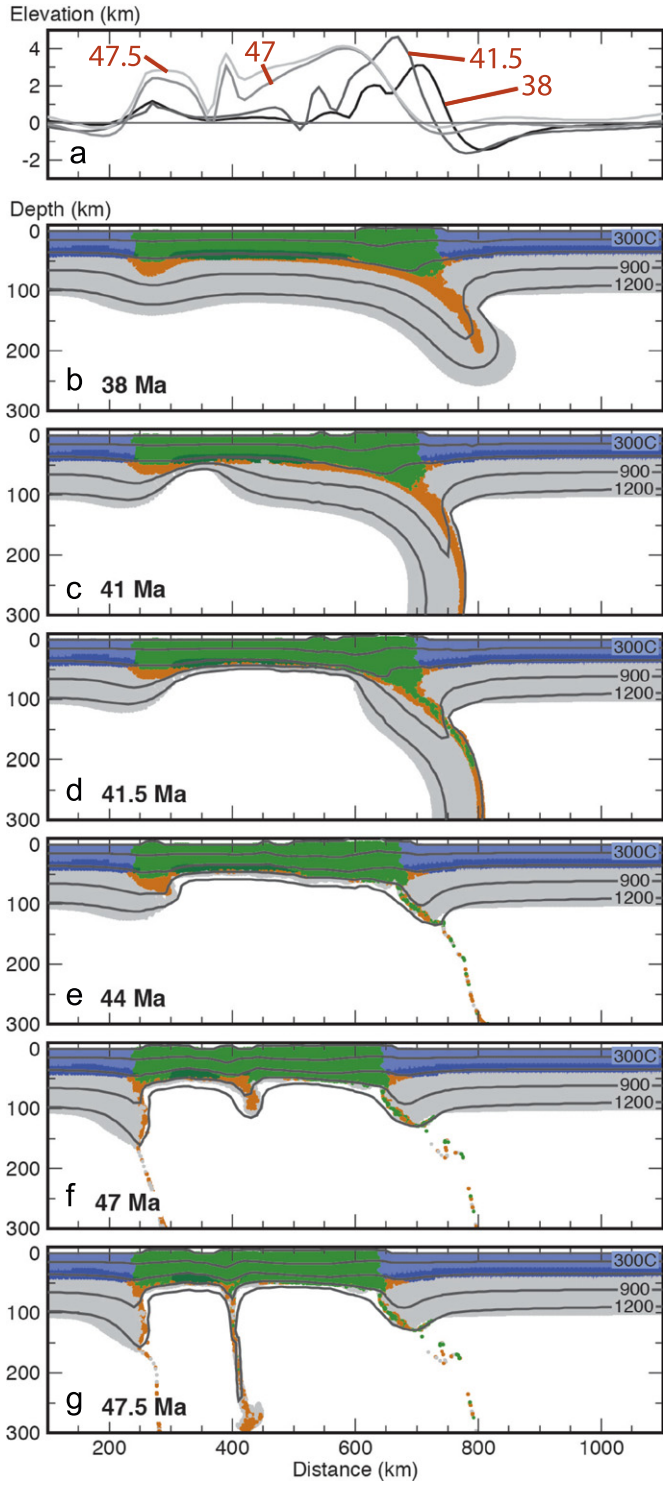

Fig. 8. The evolution of **Model 6**, in which the mantle lithosphere is five times stronger than that in **Model 2**; all other parameters are unchanged. (a) Surface topography and (b–g) model geometry at the given model times. This model undergoes stationary delamination, where the strong mantle lithosphere rapidly detaches from the crust as a coherent slab. Shortening and eclogitization of the remaining crust produces small RT-type instabilities. (a) Elevation (km), (b) 38 Ma, (c) 41 Ma, (d) 41.5 Ma, (e) 44 Ma, (f) 47 Ma and (g) 47.5 Ma.

uplift above the thickening eclogite root and underthrusting below the strong block (Fig. 8b). The underthrust lithosphere is gravitationally unstable but is too strong to undergo roll-back or break-off. Instead, the lithosphere rapidly sinks into the mantle, pulling the entire mantle lithosphere below the weak crust with it (Fig. 8c). In contrast to retreating delamination, the detachment point in this model is nearly stationary, and lithosphere is removed along a sub-horizontal shear zone in the lower crust. Delamination results in removal of orogen mantle lithosphere within ~3 Ma and affects nearly the entire width of the weak orogen, including the left side where there was no significant deformation prior to delamination (Fig. 8d). The lower crust in this area remains intact (Fig. 8e) but subsequently undergoes shortening, eclogitization and removal through RT-like drips owing to its weak rheology and high density relative to the mantle (Fig. 8f).

6. Discussion

6.1. Initiation of delamination

Our models confirm that one requirement for delamination is the presence of a weak layer that decouples the mantle lithosphere and crust (e.g., Meissner and Mooney, 1998). The initiation of delamination also requires a conduit that connects the weak layer to the sublithospheric mantle (e.g., Bird, 1979; Morency and Doin, 2004). Indeed, in Model 1, in which the lower crust is weak but does not eclogitize (Fig. 2), no conduit develops through the mantle lithosphere and no delamination occurs.

Previous studies have shown that localized convective thinning or retreat/detachment of a dense subducting plate can produce a conduit, triggering delamination (Morency and Doin, 2004; Beaumont et al., 2006; Faccenda et al., 2009; Gray and Pysklywec, 2012; Ueda et al., 2012). Our models demonstrate that lower crustal eclogitization can also induce delamination. In the models, shortening of the weak orogen is initially focused at its boundaries, leading to eclogitization of the thickening lower crust. The presence of dense eclogitized crust further localizes shortening, as also observed by Hetenyi et al. (2011). Localization occurs even if eclogite is less dense than mantle, although the degree of localization decreases at lower densities. The thick eclogitic root then starts to underthrust the incoming strong block, and delamination initiates when the underthrust lithosphere becomes gravitationally unstable and detaches from the weak crust.

The initiation of delamination can be assessed by analyzing the factors that drive and resist detachment (e.g., Bajolet et al., 2012). The driving force is provided by the negative buoyancy of the lithosphere root, which is proportional to its area (A) and density contrast ($\Delta\rho$) with respect to sublithospheric mantle (SLM). The main resisting forces are the strength of coupling between the lower crust and mantle lithosphere (given by lower crustal strength, as this is the weaker material (Fig. 1b)) and viscous resistance of the SLM. Thus, high $\Delta\rho$ and A, or weak lower crust and SLM will promote detachment.

Our model results are consistent with this relationship (Fig. 4). The mantle lithosphere is an average of ~33 kg/m^3 more dense than the shallow SLM owing to its cooler temperatures, and therefore can fully detach if the lower crust is sufficiently weak. Eclogitized lower crust, being ~750 °C cooler, is gravitationally unstable if its density is as much as 70 kg/m^3 less than SLM density. At higher densities, eclogite helps drive detachment, and therefore delamination can occur for a stronger lower crust. In addition, delamination is delayed in models with a lower eclogite density or stronger crust, suggesting that more time is needed to accumulate a sufficient area of negatively buoyant material. We did not vary SLM strength in our models, but it is expected that delamination will be inhibited with a more viscous SLM, as observed for gravitational instabilities (e.g., Molnar et al., 1998). If the conditions for detachment are not met (e.g., Model 1 with

no eclogitized crust or Model 5 with a strong crust), removal is limited to the lowermost mantle lithosphere and takes the form of RT-type drips.

6.2. Styles of delamination

When eclogitized lower crust is denser than mantle, we observe two styles of delamination (Fig. 7). At low mantle lithosphere strengths, the initial detachment event results in removal of the lithosphere root, opening a conduit between the weak lower crust and SLM. This enables further lithosphere removal through retreating delamination, with the lithosphere slab peeling from the crust and breaking into pieces as it detaches. This style is similar to post-collisional delamination observed in the models of Ueda et al. (2012). Retreating delamination requires that the detaching slab undergoes bending and roll-back during removal, driven by its negative buoyancy. As the viscous bending force is proportional to the strength of the mantle lithosphere (Bajolet et al., 2012), a weaker slab is more susceptible to bending. Over time, the length of the delaminated slab increases, resulting in greater negative buoyancy. Once the slab strength is exceeded, the slab breaks; this appears to occur through viscous necking (e.g., Duretz et al., 2012). The slab length needed for break-off decreases with decreasing mantle lithosphere strength and increasing eclogite density.

On the other hand, stronger mantle lithosphere is more resistant to bending and less likely to break. This enables a long underthrusting slab to develop. Once the negative buoyancy of the slab exceeds the strength of the lower crust, the lithosphere detaches within the weak crustal layer and the entire orogen mantle lithosphere undergoes stationary delamination, where it slides coherently into the deeper mantle at a fixed detachment point. Stationary delamination requires a pre-existing weak lower crust, which decouples the crust and strong mantle over a wide area. In contrast, retreating delamination requires weak lower crust only in the area of detachment and therefore this style of delamination may occur either in areas with a pre-existing weak crust or where a strong crust is progressively weakened through eclogitization.

A hybrid style of delamination is observed in models in which eclogite is less dense than mantle and the crust is weak (Fig. 4; Model A1 in Supplementary material). Removal initially occurs through slab roll-back and retreating delamination. However, the slab does not break, possibly due to the low eclogite density. The detaching slab grows in length and then undergoes stationary delamination that removes much of the orogen mantle lithosphere. This likely marks the point at which the negative buoyancy of the slab exceeds the strength of the lower crust.

6.3. Other factors affecting delamination (Models 7 and 8)

Several factors will modify the behaviour observed in the models. Our models have a shortening rate of 1 cm/yr, representative of the Central Andes. Fig. 9 shows the evolution of Model 7, which uses the material parameters of Model 2 but has a 2 cm/yr shortening rate, similar the Himalayas (e.g., Bilham et al., 1997). The model proceeds in a similar manner to Model 2, with the development of an eclogite root and underthrusting lithosphere (Fig. 9a), which subsequently detach (Fig. 9b). The lithosphere then stabilizes, until a second high density root forms, triggering further lithosphere removal (Fig. 9c). It appears that delamination is suppressed because the rapid incoming strong lithosphere closes the conduit produced by the first removal event. Fig. 9d–f shows the evolution of Model 8, which is the same model as

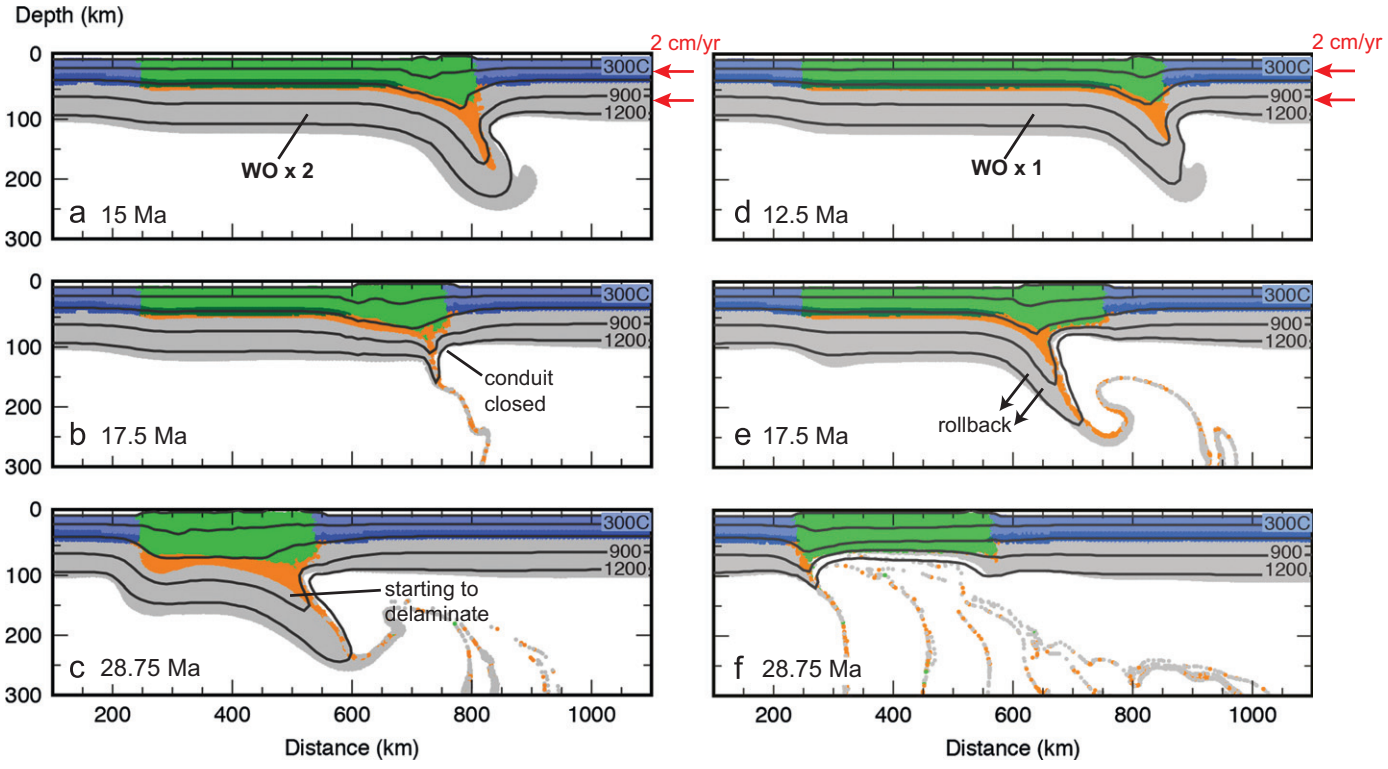

Fig. 9. (a–c) Evolution of **Model 7** with a 2 cm/yr shortening rate. All other parameters are the same as those in **Model 2**. The initial evolution is similar to that of **Model 2**, with full removal of underthrust lithosphere, but the doubled shortening rate means that this occurs in approximately half the time. The rapid incoming lithosphere then seals the conduit, preventing further delamination until a second eclogite root forms. (d–f) Evolution of **Model 8**, which is identical to **Model 7,** but with a weaker mantle lithosphere (WO × 1). After the first instability event, the weaker lithosphere rolls back quickly, allowing delamination to proceed. (a) 15 Ma, (b) 17.5 Ma, (c) 28.75 Ma, (d) 12.5 Ma, (e) 17.5 Ma and (f) 28.75 Ma.

Model 7 but the mantle lithosphere strength has been reduced by a factor of 2 (WO $\times$ 1). The initial behaviour of the two models is similar. However, after the first removal event, the weak orogen mantle lithosphere is able to roll-back quickly, enabling retreating delamination to proceed.

Other important factors include mantle lithosphere density, lithosphere thermal structure and crustal thickness. A depleted mantle lithosphere has a compositional density less than that of sublithospheric mantle (e.g., Poudjom Djomani et al., 2001) and will be less susceptible to delamination. Relative to our models, a cooler lithosphere has stronger deep crust owing to lower temperatures, which will reduce the tendency for delamination. Deep crustal temperatures also depend on crustal thickness, with thicker crust generally having higher Moho temperatures, which reduce lower crustal strength and promote delamination. Thinner crust will require more shortening before its lower crust can undergo eclogitization. This, combined with lower initial Moho temperatures, means that eclogite-induced delamination may be less likely.

6.4. Application to natural orogens

The models in this study are simplified relative to natural orogens. Nevertheless, they provide insight into orogen dynamics and demonstrate the potential role of eclogitization in lithosphere removal. It is predicted that delamination can occur in regions where eclogitized lower crust is weak and somewhat (7–8%) denser than granulitic crust, but it does not have to be more dense than mantle (Fig. 4). For a mafic composition, as inferred for continental lower crust (e.g., Christensen and Mooney, 1995), a 7 – 8% density increase corresponds to ~35–50% eclogitization, which is compatible with observations of outcrops in Norway (Austrheim et al., 1997), although there are examples of areas with less eclogitization (e.g., Leech, 2001).

Our models assume densification as lower crust enters the eclogite stability field. Kinetic hinderance will delay the density change. Model 1 (Fig. 2) is an example of complete metastability, demonstrating that delamination can be inhibited if lower crust does not transform to eclogite. Eclogite reaction kinetics are not well-constrained, although the presence of water appears to be required (e.g., Ahrens and Schubert, 1975; Austrheim, 1991; Austrheim et al., 1997), with laboratory data indicating that 1 – 2 wt% H_2O can initiate eclogitization (Leech, 2001 and references therein). Geophysical data and petrological modelling for the Tibetan Plateau suggest significant kinetic delay in eclogitization of Indian Plate lower crust (Hetenyi et al., 2007). It is proposed that eclogitization is triggered by dehydration reactions taking place >100 °C above equilibrium, at which point eclogite forms rapidly. Exhumed lower crustal rocks from the Urals, Caledonian, and Dabie-Shan orogens show partial eclogitization, where eclogites are found next to unreacted rocks that have experienced similar metamorphic conditions (e.g., Leech, 2001). In the Caledonian orogen, eclogitization tends to occur along localized fractures and shear zones, which may be pathways of fluid migration (Austrheim et al., 1997).

Delamination also requires a weak lower crust. We have tested a range of lower crustal strengths, based on a scaling of the dry Maryland diabase (DMD) rheology (Mackwell et al., 1998), which is comparable in strength to dry eclogite (Fig. 1b). DMD likely represents an upper strength limit for mafic crust, and an intermediate crust may be up to 20 times weaker (Beaumont et al., 2006). In addition, crust may be weakened through hydration. A recent study of mafic granulite containing <1 wt% water (Wang et al., 2012) shows that its strength is 10–100 times less than that of DMD (Fig. 1b), indicating that even a small amount of hydration can dramatically weaken crustal rocks. Zhang and Green (2007) suggest hydration may also lead to weakened eclogite.

For a moderate increase in crustal density during eclogitization, our models show that delamination occurs most readily for strengths of DMD $\times$ 0.1 or weaker (Fig. 4). This suggests that delamination will be limited to areas with an intermediate or partially hydrated composition. Hydration may be the most important factor, as hydration will weaken crust and facilitate eclogitization. The eclogite phase change itself may induce further weakening (e.g., Austrheim, 1991; Jackson et al., 2004). Densification and weakening of the eclogitized crust will both promote delamination, and thus there may be a link between the availability of hydrous fluids (e.g., from a nearby subducting plate), lower crustal eclogitization, and delamination. Indeed, many areas that appear to have experienced delamination are adjacent to subduction zones, including the Central Andes and East Anatolian Plateau. Conversely, either a felsic composition that does not become significantly denser upon eclogitization or kinetic hindrance due to the absence of fluids may explain the persistence of lithosphere below some orogens, such as the South Ural Mountains and the Precambrian southern Trans-Hudson orogen (Leech, 2001).

It should be noted that our models use a bulk density and rheology for lower crust in the eclogite stability field, assuming that eclogitization is widespread. In nature, eclogitization appears to occur in isolated regions that range in size from centimeters to kilometres and may be related to fluid migration (Austrheim et al., 1997; Bjornerud et al., 2002). If eclogitization is confined to local areas, it may be difficult to drive delamination, as only a small fraction of the crust will be gravitationally unstable. Further, rheological weakening associated with eclogitization will only enhance delamination if eclogitized regions are connected. Our models have relatively low resolution (2.5–10 km), and therefore higher resolution models are needed to assess the dynamics of heterogeneously eclogitized crust.

6.5. Surface observables

The main goal of our study is to understand the conditions required for eclogite-induced delamination. The models also demonstrate how delamination may be recognized in surface observations. Both retreating and stationary delamination result in full removal of orogenic mantle lithosphere, which is consistent with inferred thin lithosphere for some orogens based on seismic, gravity and elevation data (e.g., Beck and Zandt, 2002; Sengor et al., 2003; Schurr et al., 2006; Jimenez-Munt et al., 2008).

In retreating delamination, mantle lithosphere peels away from the crust, producing contemporaneous migration of crustal deformation and surface uplift (e.g., Fig. 3). During delamination, upwelling mantle and rapid crustal heating may produce magmatism that migrates across the orogen. This style of delamination has been used to explain patterns of crustal deformation and volcanism for the East Anatolian Plateau (Gogus and Pysklywec, 2008b). It may also apply in the eastern Altiplano Plateau of the Central Andes, where seismic data indicate thin lithosphere in a 100–150 km wide area (Beck and Zandt, 2002). This area was the locus of shortening from 40 to 10 Ma (Oncken et al., 2006) and has experienced over 1.5 km of uplift since 12 Ma and volcanism associated with the Miocene Los Frailes complex (Garzione et al., 2008; Kay and Coira, 2009). This history is consistent with the development of an eclogitic root, followed by its removal in the Late Miocene. This may be a local area of lithosphere removal or these events may mark the initiation of retreating delamination, which has not yet affected the central Altiplano (Beck and Zandt, 2002).

In stationary delamination, shortening and uplift are confined to one area, but lithosphere is rapidly removed over a wider area, determined by the presence of weak lower crust (e.g., Fig. 8). Following removal, the full width of the orogen experiences deformation, uplift and crustal heating, which may produce widespread magmatism. The surface topography in this model

bears some resemblance to topography across the Eastern Carpathians, where Miocene shortening was localized in the mountain belt, but proposed lithosphere removal at 11 Ma affected a wider area (Fillerup et al., 2010). This style of removal may also have occurred in the Puna Plateau, which is an area characterized by thin lithosphere (Schurr et al., 2006) and extensive volcanism in the last 10 Ma (Kay and Kay, 1993; Kay and Coira, 2009).

7. Conclusions

Geophysical and geological observations indicate thin mantle lithosphere for many orogens. Previous studies have argued for the importance of eclogitized lower crust in triggering lithosphere removal through delamination (e.g., Kay and Kay, 1993). Our models provide a systematic examination of the effect of metamorphic eclogitization for an actively shortening orogen. The following conclusions may be drawn:

(1) Through eclogitization, the density of the deep crust increases. Even a modest density increase produces localized shortening, enhancing the development of a thick root of eclogitized crust and mantle lithosphere. Gravitational instability of this root leads to lithosphere removal.
(2) The strength of the eclogitized crust is an important control on lithosphere removal. If the deep crust is strong, the crust and mantle are coupled, and removal is limited to the lowermost lithosphere. Conversely, if eclogitized crust is weak, the entire mantle lithosphere can be removed through delamination. This can occur if eclogitized crust is less dense than the mantle, as long as the crust is weak enough to allow detachment of the mantle lithosphere. Higher density eclogite helps drive delamination.
(3) For the range of eclogite densities tested in this study, delamination occurs only if the eclogitized lower crust is significantly weaker than the strength of dry eclogite determined in laboratory studies. This appears to require the presence of a small amount of hydrous fluids, which trigger the eclogite phase change and reduce crustal strength. In nature, eclogitization may occur in isolated areas associated with fluid migration; if eclogitization is strongly localized, delamination may be suppressed.
(4) Two styles of delamination are observed. Weak mantle lithosphere peels away from the crust at a retreating detachment point, whereas strong mantle lithosphere detaches from the crust and slides into the mantle as a coherent slab at a nearly stationary detachment point. Both styles lead to complete removal of orogenic mantle lithosphere but exhibit differences in the evolution of crustal deformation, surface topography and magmatism.

Acknowledgements

Numerical models in this study use the SOPALE modelling code, developed under the direction of Dr. Christopher Beaumont at Dalhousie University (Halifax, Canada). We thank Manuele Faccenda, Mary Leech, Boris Kaus, and two anonymous reviewers for constructive comments on earlier versions of this manuscript. This work is supported by research grants from the Exxon Mobil Upstream Research Company and the NSERC.

Appendix A. Supplementary material

Supplementary data associated with this article can be found in the online version at http://dx.doi.org/10.1016/j.epsl.2012.09.056.

References

Ahrens, T.J., Schubert, G., 1975. Gabbro-eclogite reaction rate and its geophysical significance. Rev. Geophys. 13, 383–400.
Austrheim, H., 1991. Eclogite formation and dynamics of crustal roots under continental collision zones. Terra Nova 3, 492–499.
Austrheim, H., Erambert, M., Engvik, A.K., 1997. Processing of crust in the root of the Caledonian continental collision zone: the role of eclogitization. Tectonophysics 273, 129–153.
Bajolet, F., Galeano, J., Funiciello, F., Moroni, M., Nagredo, A.M., Faccenna, C., 2012. Continental delamination: insights from laboratory models. Geochem. Geophys. Geosyst. 13, Q02009, http://dx.doi.org/10.1029/2011GC003896.
Beaumont, C., Nguyen, M.H., Jamieson, R.A., Ellis, S., 2006. Crustal flow modes in large hot orogens. In: Law, R.D., Searle, M.P., Godin, L. (Eds.), Channel Flow, Ductile Extrusion, and Exhumation of Lower-Mid Crust in Continental Collision Zones, 268. Special Publications, Geological Society London, pp. 91–145.
Beck, S.L., Zandt, G., 2002. The nature of orogenic crust in the central Andes. J. Geophys. Res., 107, http://dx.doi.org/10.1029/2000JB000124.
Bilham, R., Larson, K., Freymueller, J., 1997. GPS measurements of present-day convergence across the Nepal Himalaya. Nature 386, 61–64.
Bird, P., 1979. Continental delamination and the Colorado Plateau. J. Geophys. Res. 84, 7561–7571.
Bjornerud, M.G., Austrheim, H., Lund, M.G., 2002. Processes leading to eclogitization (densification) of subducted and tectonically buried crust. J. Geophys. Res. 107, 2252, http://dx.doi.org/10.1029/2001JB000527.
Bousquet, R., Goffe, B., Henry, P., Le Pichon, X., Chopin, C., 1997. Kinematic, thermal and petrological model of the Central Alps: lepontine metamorphism in the upper crust and eclogitisation of the lower crust. Tectonophysics 273, 105–127.
Buck, W.R., Toksoz, M.N., 1983. Thermal effects of continental collisions: thickening a variable viscosity lithosphere. Tectonophysics 100, 53–69.
Christensen, N.I., Mooney, W.D., 1995. Seismic velocity structure and composition of the continental crust: a global view. J. Geophys. Res. 100, 9761–9788.
Conrad, C.P., Molnar, P., 1999. Convective instability of a boundary layer with temperature- and strain-dependent viscosity in terms of 'available buoyancy'. Geophys. J. Int. 139, 51–68.
Currie, C.A., Beaumont, C., 2011. Are diamond-bearing Cretaceous kimberlites related to low-angle subduction beneath western North America? Earth Planet. Sci. Lett. 303, 59–70.
Doin, M.-P., Henry, P., 2001. Subduction initiation and continental crust recycling: the roles of rheology and eclogitization. Tectonophysics 342, 163–191.
Ducea, M., Saleeby, J., 1998. A case for delamination of the deep batholithic crust beneath the Sierra Nevada, California. Int. Geol. Rev. 40, 78–93.
Duretz, T., Schmalholz, S.M., Gerya, T.V., 2012. Dynamics of slab detachment. Geochem. Geophys. Geosyst. 13, Q03020, http://dx.doi.org/10.1029/2011GC004024.
Ellis, S., Beaumont, C., Jamieson, R.A., Quinlan, G., 1998. Continental collision including a weak zone: the vise model and its application to the Newfoundland Appalachians. Can. J. Earth Sci. 35, 1323–1346.
England, P., Houseman, G., 1989. Extension during continental convergence, with application to the Tibetan Plateau. J. Geophys. Res. 94, 17561–17579.
Faccenda, M., Minelli, G., Gerya, T.V., 2009. Coupled and decoupled regimes of continental collision: numerical modeling. Earth Planet. Sci. Lett. 278, 337–349.
Fillerup, M.A., Knapp, J.H., Knapp, C.C., Raileanu, V., 2010. Mantle earthquakes in the absence of subducton? Continental delamination in the Romanian Carpathians. Lithosphere 2, 333–340.
Fullsack, P., 1995. An arbitrary Lagrangian–Eulerian formulation for creeping flows and applications in tectonic models. Geophys. J. Int. 120, 1–23.
Garzione, C.N., Hoke, G.D., Libarkin, J.C., Withers, S., MacFadden, B., Eiler, J., Ghosh, P., Mulch, A., 2008. Rise of the Andes. Science 320, 1304–1307.
Gleason, G.C., Tullis, J., 1995. A flow law for dislocation creep of quartz aggregates determined with the molten salt cell. Tectonophysics 247, 1–23.
Gogus, O.H., Pysklywec, R.N., 2008a. Near surface diagnostics of dripping and delaminating lithosphere. J. Geophys. Res. 113, B11404, http://dx.doi.org/10.1029/2007JB005123.
Gogus, O.H., Pysklywec, R.N., 2008b. Mantle lithosphere delamination driving plateau uplift and synconvergent extension in eastern Anatolia. Geology 36, 723–726.
Gray, R., Pysklywec, R.N., 2012. Geodynamic models of mature continental collision: evolution of an orogen from lithospheric subduction to continental retreat/delamination. J. Geophys. Res. 117, B03408, http://dx.doi.org/10.1029/2011JB008692.
Gutierrez-Alonso, G., Murphy, J.B., Fernandez-Suarez, J., Weil, A.B., Franco, M.P., Gonzalo, J.C., 2011. Lithospheric delamination in the core of Pangea: Sm-Nd insights from the Iberian mantle. Geology 39, 155–158.
Hacker, B.R., Abers, G.A., Peacock, S.M., 2003. Subduction factory 1. Theoretical mineralogy, densities, seismic wave speeds, and H_2O contents. J. Geophys. Res. 108, B12029, http://dx.doi.org/10.1029/2001JB001127.
Hetenyi, G., Cattin, R., Brunet, F., Bollinger, L., Vergne, J., Nabelek, J.L., Diament, M., 2007. Density distribution of the India plate beneath the Tibetan plateau: geophysical and petrological constraints on the kinetics of lower-crustal eclogitization. Earth Planet. Sci. Lett. 264, 226–244.
Hetenyi, G., Godard, V., Cattin, R., Connolly, J.A.D., 2011. Incorporating metamorphism in geodynamic models: the mass conservation problem. Geophys. J. Int. 186, 6–10.

Houseman, G.A., McKenzie, D.P., Molnar, P., 1981. Convective instability of a thickened boundary layer and its relevance for the thermal evolution of continental convergence belts. J. Geophys. Res. 86, 6115–6132.
Jackson, J.A., Austrheim, H., McKenzie, D., Priestley, K., 2004. Metastability, mechanical strength, and the support of mountain belts. Geology 32, 625–628.
Jimenez-Munt, I., Fernàndez, M., Vergés, J., Platt, J.P., 2008. Lithosphere structure underneath the Tibetan Plateau inferred from elevation, gravity and geoid anomalies. Earth Planet. Sci. Lett. 267, 276–289.
Jin, Z.M., Zhang, J., Green, H.W., Jin, S., 2001. Eclogite rheology: implications for subducted lithosphere. Geology 2, 667–670.
Jull, M., Kelemen, P.B., 2001. On the conditions for lower crustal convective instability. J. Geophys. Res. 106, 6423–6446.
Karato, S.I., Wu, P., 1993. Rheology of the upper mantle: a synthesis. Science 260, 771–778.
Kay, S.M., Coira, B.L., 2009. Shallowing and steepening subduction zones, continental lithospheric loss, magmatism, and crustal flow under the Central Andean Altiplano–Puna Plateau. Geol. Soc. Am. Mem. 204, 229–259.
Kay, R.W., Kay, S.M., 1993. Delamination and delamination magmatism. Tectonophysics 219, 177–189.
Keskin, M., 2003. Magma generation by slab steepening and breakoff beneath a subduction-accretion complex: an alternative model for collision-related volcanism in Eastern Anatolia, Turkey. Geophys. Res. Lett. 30, 8046, http://dx.doi.org/10.1029/2003GL018019.
Knapp, J.H., Knapp, C.C., Raileanu, V., Matenco, L., Mocanu, V., Dinu, C., 2005. Crustal constraints on the origin of mantle seismicity in the Vrancea Zone, Romania: the case for active continental delamination. Tectonophysics 410, 311–323.
Leech, M.L., 2001. Arrested orogenic development: eclogitization, delamination, and tectonic collapse. Earth Planet. Sci. Lett. 185, 149–159.
Le Pourheit, L., Gurnis, M., Saleeby, J., 2006. Mantle instability beneath the Sierra Nevada Mountains in California and Death Valley extension. Earth Planet. Sci. Lett. 251, 104–119.
Mackwell, S.J., Zimmerman, M.E., Kohlstedt, D.L., 1998. High temperature deformation of dry diabase with application to tectonics on Venus. J. Geophys. Res. 103, 975–984.
Meissner, R.O., Mooney, W.D., 1998. Weakness of the lower continental crust; a condition for delamination, uplift, and escape. Tectonophysics 296, 47–60.
Molnar, P., Tapponnier, P., 1981. A possible dependence of tectonic strength on the age of the crust in Asia. Earth Planet. Sci. Lett. 52, 107–114.
Molnar, P., Houseman, G.A., Conrad, C.P., 1998. Rayleigh–Taylor instability and convective thinning of mechanically thickened lithosphere: effects of non-linear viscosity decreasing exponentially with depth and of horizontal shortening of the layer. Geophys. J. Int. 133, 568–584.
Morency, C., Doin, M.-P., 2004. Numerical simulations of the mantle lithosphere delamination. J. Geophys. Res. 109, B03410, http://dx.doi.org/10.1029/2003JB002414.
Oncken, O., Hindle, D., Kley, J., Elger, K., Victor, P., Schemmann, K., 2006. Deformation of the Central Andean upper plate system—facts, fiction and constraints for plateau models. In: Oncken, Ol., Chong, G., Franz, G., Giese, P., Gotze, H.J., Ramos, V.A., Strecker, M.R., Wigger, P. (Eds.), The Andes: Active Subduction Orogeny. Springer, pp. 3–27.
Poudjom Djomani, Y.H., O'Reilly, S.Y., Griffin, W.L., Morgan, P., 2001. The density structure of subcontinental mantle through time. Earth Planet. Sci. Lett. 184, 605–621.
Pysklywec, R.N., Beaumont, C., 2004. Intraplate tectonics: feedback between radioactive thermal weakening and crustal deformation driven by mantle lithosphere instabilities. Earth Planet. Sci. Lett. 221, 275–292.
Schott, B., Schmeling, H., 1998. Delamination and detachment of a lithospheric root. Tectonophysics 296, 225–247.
Schurr, B., Rietbrock, A., Asch, G., Kind, R., Oncken, O., 2006. Evidence for lithospheric detachment in the central Andes from local earthquake tomography. Tectonophysics 415, 203–223.
Sengor, A.M.C., Özeren, S., Genc, T., Zor, E., 2003. East Anatolian high plateau as a mantle-supported, north–south shortened domal structure. Geophys. Res. Lett. 30, 8045, http://dx.doi.org/10.1029/2003GL017858.
Sobolev, S.V., Babeyko, A.Y., 2005. What drives orogeny in the Andes? Geology 33, 617–620.
Ueda, K., Gerya, T.V., Burg, J.-P., 2012. Delamination in collisional orogens: thermomechanical modeling. J. Geophys. Res. 117, B08202, http://dx.doi.org/10.1029/2012JB009144.
Valera, J.L., Negredo, A.M., Jimenez-Munt, L., 2011. Deep and near-surface consequences of root removal by asymmetric continental delamination. Tectonophysics 502, 257–265.
Wang, Y.F., Zhang, J.F., Jin, Z.M., Green II, H.W., 2012. Mafic granulite rheology: implications for a weak continental lower crust. Earth Planet. Sci. Lett. 353-354, 99–107.
Warren, C.J., Beaumont, C., Jamieson, R.A., 2008. Formation and exhumation of ultra-high-pressure rocks during continental collision: role of detachment in the subduction channel. Geochem. Geophys. Geosyst. 9, Q04019, http://dx.doi.org/10.1029/2007GC001839.
Willett, S.D., 1999. Rheological dependence of extension in wedge models of convergent orogens. Tectonophysics 305, 419–435.
Zhang, J., Green II, H.W., 2007. Experimental investigation of eclogite rheology and its fabrics at high temperature and pressure. J. Metamorphic Geol. 25, 97–115.